Modelling Radon Entry into Houses with Basements: Model Description and Verification

K.L. Revzan[*], W.J. Fisk[*], and A.J. Gadgil[*]
Lawrence Berkeley Laboratory, USA

Abstract

We model radon entry into basements using a previously developed three-dimensional steady-state finite difference model that has been modified in the following ways: first, cylindrical coordinates are used to take advantage of the symmetry of the problem in the horizontal plane, thereby increasing resolution and computing efficiency without significant loss of generality; second, the configuration of the basement has been made more realistic by incorporating the concrete footer which supports the basement walls and floor; third, a quadratic relationship between the pressure and flow in the L-shaped gap between slab, footer, and wall has been employed; and fourth, the natural convection of the soil gas which follows from the heating of the basement in winter has been taken into account. The temperature field in the soil is determined from the equation of energy conservation, using the basement, surface, and deep-soil temperatures as boundary conditions. The pressure field is determined from Darcy's law and the equation of mass conservation (continuity), assuming that there is no flow across any boundary except the soil surface (atmospheric pressure) and the opening in the basement shell (fixed pressure). Since the energy conservation equation includes both heat advection and conduction, the temperature and pressure equations must be coupled. After the pressure and temperature fields have been obtained, the velocity field is found from Darcy's law. Finally, the radon concentration field is found from the equation of mass-transport, assuming that diffusive entry through openings may be neglected. The convective radon entry rate through the opening or openings is then calculated. In this paper we describe the modified model, compare the predicted radon entry rates with and without the consideration of thermal convection, and compare the predicted rates with rates determined from data from seven houses in the Spokane River valley of Washington and Idaho. Although the predicted rate is much lower than the mean of the rates determined from measurements, errors in the measurement of soil permeability and variations in the permeability of the area immediately under the basement slab, which has a significant influence on the pressure field, can account for the range of entry rates inferred from the data.

Introduction

The primary source of radon in houses with high indoor concentrations is, in most cases, the surrounding soil; the primary means of entry is generally the passage of soil-gas through cracks or other gaps in the building shell (Nero, 1988) or through permeable sub-surface walls (Garbesi and Sextro, 1990). In houses with basements, for which the length of the soil-gas path from soil surface to entry point may be long and the pore-space radon concentration consequently elevated, radon entry rates may be particularly high. The soil-gas flow rate is primarily dependent on the permeability of the soil, on

the nature of openings in the building shell, and on the degree of basement depressurization. The radon concentration in the soil is dependent on the soil gas velocity, the radium content, porosity, density, and emanating fraction of the soil, the diffusivity of radon in the soil, and the depth.

A model amenable to closed-form solutions can provide only a crude representation of the problem. One such model is described by Mowris and Fisk (1987) and by Nazaroff (1988b). A linear crack in the basement slab is represented in bipolar coordinates by a cylinder embedded in a homogeneous semi-infinite medium; the soil surface is represented by a plane parallel to the axis of the cylinder. The basement itself is not modelled. Darcy's law and the continuity equation, which together describe soil-gas transport, reduce to the Laplace equation for the pressure field; this equation has a series solution. The mass-transport equation without diffusion may then be solved for the radon concentration field, assuming a fixed concentration at infinite radius, and the two solutions combined to give the radon entry rate at the cylinder. This model gives an indication of the dependence of the entry rate on basement pressure and soil permeability when the soil is homogeneous, but it cannot represent the basement-soil boundary correctly, nor can it deal with inhomogeneous soils.

Recognition of the limitations of closed-form models has led to the development of numerical models, such as the two-dimensional models of Dimbylow (1987) and of Mowris and Fisk (1987), and the three-dimensional model of Loureiro (1987) and Loureiro et al. (1990), which are able to deal with irregular boundaries and arbitrary boundary conditions. Here, steady-state solutions of the generalized Laplace equation and the mass-transport equation are given in Cartesian coordinates for a region comprising a quadrant of a basement and a block of soil large enough that a further increase in size produces an insignificant change in the soil-gas and radon entry rates. The basement walls and slab and the outer limits of the soil block are treated as no-flow boundaries, while the soil surface is a boundary at atmospheric pressure and zero radon concentration. In the Loureiro model, the pressure, soil-gas velocity, and radon concentration in peripheral gaps (of rectangular cross-section) in the basement slab are modelled analytically and the results adjusted to match those of the numerical solution at the soil-gap interface. The variability of the soil characteristics is essentially unlimited, although variation on a fine scale may lead to an excessively large number of control volumes, long solution times, and large computing costs.

In this paper, we describe a steady-state numerical model based on that of Loureiro, but one that takes advantage of the symmetry of the problem in the horizontal plane by using cylindrical coordinates. There is a loss of generality in that only central and peripheral openings in the basement shell can be modelled, but these are, in fact, the only types considered in earlier work. The model has also been modified so that the concrete footer that normally supports the wall and slab is included, giving the slab-footer-wall gap an L-shape. The boundary conditions at the soil-gap interface have been altered in order to take this shape into consideration. This gap, which is considered to be an important source of indoor radon in many houses, is the only opening in the building shell discussed in detail in this paper; for a description of models with alternative or additional openings, see Revzan and Fisk (1990) and Garbesi and Sextro (1990). The Loureiro model neglects the circulation of soil gas which occurs in winter and is caused by the presence of a heated basement; we incorporate this circulation into the model and demonstrate that buoyancy forces acting on soil gas may be an important factor in radon entry. Finally, to verify the numerical model to the limited extent possible, we compare the predictions of the

model for the Valley of Washi from seven hou ence of soil char discussed in deta

Model Descr

The region to subsurface part o the surrounding the basement so gap between the and the walls. (G tions are discus 1990.) Assuming walls and gaps d can be modelled loss of corner eff be unimportant. house draws soil of adjacent houses surization, and th

10 m

rates. The basement
ter limits of the soil
to-flow boundaries,
a boundary at atmo-
to radon concentra-
model, the pressure,
on concentration in
gular cross-section)
modelled analytical-
d to match those of
: the soil-gap inter-
e soil characteristics
although variation
l to an excessively
olumes, long solu-
uting costs.
ribe a steady-state
n that of Loureiro,
ntage of the sym-
e horizontal plane
linates. There is a
only central and
he basement shell
e are, in fact, the
earlier work. The
lified so that the
ally supports the
ving the slab-foo-
he boundary con-
face have been al-
hape into consid-
considered to be
ndoor radon in
opening in the
n detail in this
of models with
enings, see Rev-
besi and Sextro
neglects the cir-
occurs in winter
nce of a heated
this circulation
trate that buoy-
may be an im-
Finally, to veri-
e limited extent
edictions of the

model for the soil of the Spokane River Valley of Washington and Idaho with data from seven houses in that area. The influence of soil characteristics on radon entry is discussed in detail in Revzan (1990).
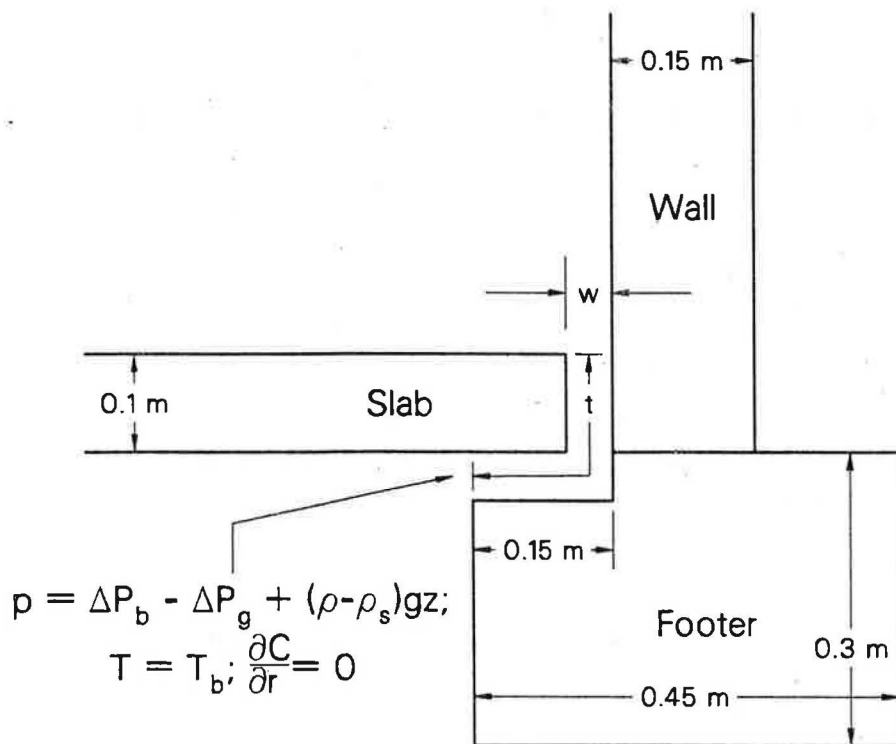
Model Description

The region to be modelled comprises the subsurface part of a basement and a block of the surrounding soil. Air is assumed to enter the basement solely through an L-shaped gap between the foundation footer, the slab, and the walls. (Gaps and cracks at other locations are discussed in Revzan and Fisk, 1990.) Assuming that the cross-section of the walls and gaps does not vary, the basement can be modelled as a cylinder with only the loss of corner effects, which will be shown to be unimportant. The region from which a house draws soil gas depends on the position of adjacent houses, the extent of their depressurization, and the characteristics of the soil.

The exact boundaries of this region are likely to be important in particular cases, but in general, the soil block may be represented as well by a cylinder as by a box. The entire region may therefore be modelled in cylindrical coordinates, which permits greater resolution, shorter solution time (with lower cost), or a combination of the two. A vertical cross-section of the region, with the dimensions used in this paper, is shown in Figure 1. A detail of the cross-section of the basement area, with the width of the gap greatly exaggerated, is shown in Figure 2. In this paper, the gap width, w, is assumed to be 0.003 m and the thickness, t, to be 0.25 m.

Fig. 1 Vertical cross-section of the region modelled; the shaded areas are the wall, slab, and footer. The boundary conditions for the temperature (T), disturbance pressure (p), and radon concentration (C) fields at the soil surface and at the outer and lower soil boundaries are shown in the appropriate locations. The definition of the pressure p is also shown; P is the absolute pressure, P_A is the atmospheric pressure, ρ is the air density and ρ_s is its value at the lower soil boundary, g is the acceleration of gravity, and z is the vertical coordinate, taken positive downward.

$$T = T_o; \quad p = 0; \quad C = 0$$

2 m

10 m

5 m

$$p(r,z) = P(r,z) - P_A - \rho_s gz$$

$$\frac{\partial T}{\partial r} = 0$$

$$\frac{\partial p}{\partial r} = 0$$

$$\frac{\partial C}{\partial r} = 0$$

10 m
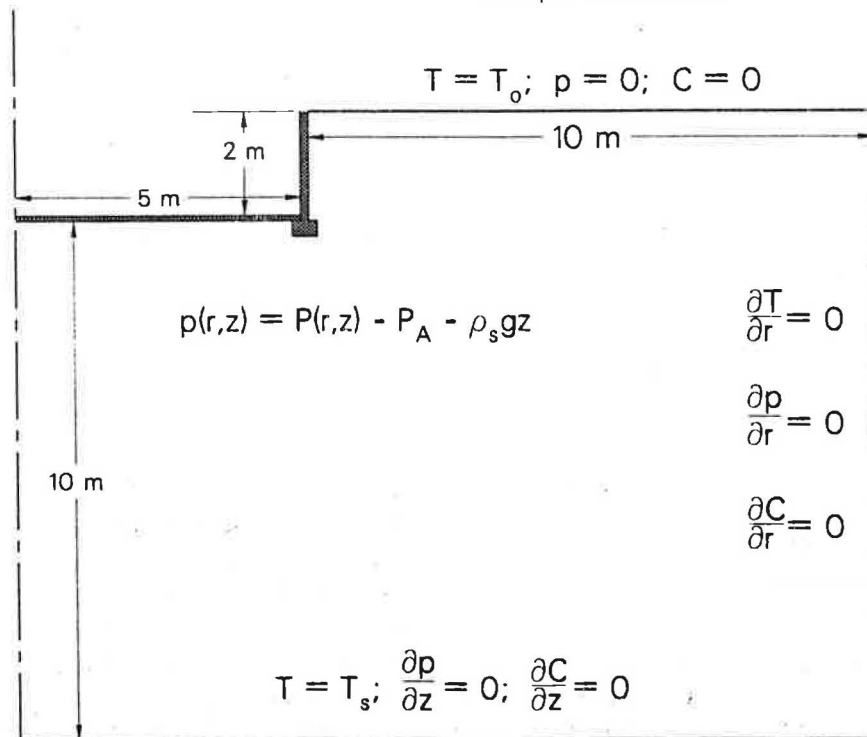
$$T = T_s; \quad \frac{\partial p}{\partial z} = 0; \quad \frac{\partial C}{\partial z} = 0$$

Fig. 2 Detail of the vertical cross-section of the region modelled. The widths of the slab-footer and slab-wall gaps are shown greatly exaggerated. The boundary conditions at the vertical and horizontal concrete surfaces are given below the figure. For the temperature and concentration fields, the vertical boundary conditions also apply at the soil-gap interface; the boundary condition for the pressure at the interface is shown just below the basement slab. T_b is the basement temperature, ΔP_b is the pressure difference between the basement and the outside, ΔP_g is the pressure difference between the basement and the soil-gap interface, ρ is the soil-gas (air) density generally, ρ_s is the soil-gas density at the lower soil boundary, w is the gap width and t the gap thickness. The definition of the pressure p is given in the text and in Figure 1.

The model comprises three differential equations. First, the temperature field in the soil is found from the steady-state energy conservation equation (assuming thermal equilibrium between the solid as gaseous phases of the soil [Bejan, 1984; Ene and Polisevski, 1987]),

$$\frac{1}{\rho_0}\nabla \cdot \left[\rho(r, z)\vec{v}(r, z)T(r, z)\right] = \nabla \cdot \left[\alpha(r, z)\nabla T(r, z)\right] \quad (1)$$

where ρ_0 is the density of air at 0 °C, T is the temperature, α is the thermal diffusivity at 0° C, and $\vec{v}$ is the soil-gas velocity. We assume that $\alpha = 5\times10^{-7}$ m^2 s^{-1} throughout the soil (Oke, 1987). The temperature is fixed at T_b at the outside of the basement, including the soil-gap interface, at T_o at the soil surface ("outside", $z=0$), and at T_s at the lower limit

of the soil ($z =$
mit of the soil
sumed to repr
two houses, so
i.e., the normal
These bounda
Figures 1 and 2
determined by
fields, the hea
tions must be
practical impo
tion is negligib
so that the left-
be set to zero a
termined indep
The circumstan
tion is signific
following sectio
Next, the pr
generalization c

$$\vec{v}(r, z) = \frac{k(r, z)}{\mu}$$

where k is the
is assumed to b
air (1.8×10^{-5} kg
sure, ρ the dens
gravity, and $\hat{z}$ t
tion, taken posi
tures of interes
upon T is given

$$\rho(r, z) = \rho_0\left[1-\beta\right]$$

where T is in °
0 °C (1.293 kg m
thermal expans
equal to 1/273 °
it is customary
sure by subtrac
tic pressures fr
density of air w
to choose a ref
trary, rather tha
sion for the sta
tions are some
ence is either ρ

of the soil (z = 12.1 m, Figure 1). The outer limit of the soil (r = 15.15 m, Figure 1) is presumed to represent the boundary between two houses, so that here there is no heat flow, i.e., the normal derivative of T must vanish. These boundary conditions are shown in Figures 1 and 2. Since the soil-gas velocity is determined by the pressure and temperature fields, the heat-transfer and pressure equations must be coupled. In many cases of practical importance, however, heat advection is negligible with respect to conduction, so that the left-hand side of Equation 1 may be set to zero and the temperature field determined independently of the pressure field. The circumstances under which heat advection is significant will be described in the following section.

Next, the pressure field is found from a generalization of Darcy's law, i.e.,

$$\vec{v}(r, z) = \frac{k(r, z)}{\mu} \left[\rho(r, z)g\hat{z} - \nabla P(r, z) \right] \qquad (2)$$

where k is the permeability of the soil, which is assumed to be isotropic, μ the viscosity of air (1.8×10^{-5} kg m^{-1} s^{-1}), P the absolute pressure, ρ the density of air, g the acceleration of gravity, and $\hat{z}$ the unit vector in the z-direction, taken positive downward. For temperatures of interest here, the dependence of ρ upon T is given by

$$\rho(r, z) = \rho_0 \left[1 - \beta T(r, z) \right] \qquad (3)$$

where T is in °C, ρ_0 is the density of air at 0 °C (1.293 kg m^{-3}), and β is the coefficient of thermal expansion, which is approximately equal to 1/273 °C^{-1}. For isothermal problems, it is customary to define a disturbance pressure by subtracting the atmospheric and static pressures from P. In our case, since the density of air varies with z, it is convenient to choose a reference density, which is arbitrary, rather than to use the integral expression for the static pressure. Boundary conditions are somewhat simplified if the reference is either ρ_b, the density where T = T_b,

or ρ_s, the density where T = T_s. We choose the latter density and define the disturbance pressure, p, by the equation

$$p(r, z) = P(r, z) - P_A - \rho_s gz \qquad (4)$$

where P_A is the atmospheric pressure, assumed constant in a steady-state model. Combining Equations 2, 3, and 4 gives

$$\vec{v}(r, z) = \frac{k(r, z)}{\mu} \left[\rho_0 g\beta[T_s - T(r, z)]\hat{z} - \nabla p(r, z) \right] \qquad (5)$$

The first term on the right-hand side of this equation vanishes at the lower boundary of the soil, i.e., when $T(r, z_s) = T_s$, so that the boundary condition here becomes simply a zero normal derivative. This convenience is the justification for the choice of ρ_s as the reference density.

The equation of conservation of mass (continuity) is

$$\nabla \cdot \left[\rho(r, z)\vec{v}(r, z) \right] = 0 \qquad (6)$$

Combining Equations 5 and 6, we have the second equation of the model, i.e.,

$$\nabla \cdot \left\{ \frac{\rho(r, z)k(r, z)}{\mu} \left[\nabla p(r, z) + \rho_0 g\beta[T(r, z) - T_s]\hat{z} \right] \right\} = 0 \qquad (7)$$

This equation must be solved in conjunction with Equation 1 when thermal convection is significant.

The boundaries for the solution of Equation 7 are the outer limit of the soil block in the r-direction, the soil surface and the lower limit of the soil block in the z-direction, and either the inner or outer basement surfaces, including the opening. If the inner basement surface is chosen as a boundary, the entire gap between slab and footer and wall and footer must be included in the problem. The gap width is typically four orders of magnitude smaller than the soil block size and the soil gas must change direction as it passes through the gap, so that the control

volumes must be made very small in this region. As a result, computation time is high In actual construction, moreover, the gap has irregular walls, so that it is not well represented by the model. Consequently, it is best to take the boundaries of the problem to be the outside surfaces of the basement and footer, including the mouth (soil-gap interface) of the slab-footer gap, and to treat the question of the gap itself separately. With these boundaries, radon entry by diffusion through concrete is neglected; this subject has been treated by Zapalac (1983). The question of radon entry through permeable walls is also neglected here, although the model is capable of treating the subject with only slight modifications. Garbesi and Sextro (1990) discuss soil-gas entry through permeable walls, but do not deal with radon entry *per se*.

Given these assumptions, the normal velocity must vanish at all concrete surfaces and at the outer and lower limits of the soil and the pressure must be fixed at the soil surface and the soil-gap interface. At vertical concrete surfaces and at the outer soil boundary, the vanishing of the normal velocity is equivalent to a zero normal pressure derivative. At horizontal concrete surfaces and at the lower soil boundary, Equation 5 gives

$$\frac{\partial p(r, z_s)}{\partial z} - \rho_0 \beta g [T_s - T(r, z_s)] = 0 \tag{8}$$

where z_s is the position of the surface of interest. At the lower soil boundary, this equation reduces to a vanishing normal derivative of p. At the soil surface, $z = 0$, $P = P_A$ and Equation 4 gives the boundary condition $p(r,0) = 0$. The boundary conditions at the three soil boundaries are shown in Figure 1.

The pressure at the soil-gap interface is determined by the basement pressure and the pressure drop across the gap. In winter, temperature differences between a house and the outside, the effect of wind, and the operation of heating, ventilation, and air-con-

ditioning systems produce a basement pressure which is generally lower than P_A (Feustel and Sherman, 1989; Sherman et al., 1979; Revzan et al., 1988; Revzan, 1989). The difference between the pressure at the basement side of the slab-wall gap and P_A, corrected for the static pressure difference, is written as ΔP_b. The pressure drop across the gap, ΔP_g, is determined from an algorithm due to Baker, et al. (1989):

$$|\Delta P_g| = \frac{12\mu t}{w^2} |\vec{v}| + \frac{\rho(1.5 + n)}{2} v^2 \tag{9}$$

Here, t and w are, respectively, the thickness and width of the opening (see Figure 2), v is the average speed of air through the opening, i.e., the flow rate through the opening divided by the area, and n is the number of bends in the opening. Assuming that the temperature is constant inside the gap, so that there is no thermally-induced pressure difference between the basement and soil sides, the disturbance pressure at the soil-gap interface is then

$$p(r_g, z) = \Delta P_b + |\Delta P_g| + \rho_0 \beta g (T_s - T_b) z \tag{10}$$

where r_g is the radial coordinate of the soil side of the gap. The boundary conditions at the basement may be clarified by examining Figure 2.

Having found a solution to Equation 7, we may determine the soil-gas velocity from Equation 5. The soil-gas entry rate, E_s, is then given by

$$E_s = \int_\Sigma \vec{v}(r_g, z) \cdot d\vec{\sigma}(r_g, z) \tag{11}$$

where $\vec{\sigma}$ is an element of the area of the soil-gap interface and $\sum$ indicates an integral over the entire interface area.

Finally, the radon concentration in the soil gas, C, is determined from

$$\nabla \cdot \left[\vec{v}(r, z) C(r, z) \right] = \nabla \cdot \left[D(r, z) \nabla C(r, z) \right]$$
$$- \varepsilon(r, z) \lambda C(r, z) + \varepsilon(r, z) S(r, z) \tag{12}$$

where D is t soil, λ the rad ity of the soil, don into the s In this paper homogeneous 0.5 (Nazaroff, deal with spat values of D, ε, wet conditions solution of Eq for Equation face. At the s because radon typically high mosphere, th soil-surface co fect on the res try by diffusio compared to the radon con the gap is equ i.e., the norm the soil-gap may be made, side an openi but the effect rate is negligi is high enoug concentrations al., 1990).

The radon from the soil is given by

$$C_\infty = \frac{S}{\lambda}$$

Since this pap characteristics source strength that results previously de tion to Equat radon entry ra

$$E_r = \frac{1}{C_\infty} \int_\Sigma C$$

e a basement pres-
v lower than P_A
39; Sherman et al.,
Revzan, 1989). The
essure at the base-
gap and P_A, correc-
difference, is writ-
rop across the gap,
a algorithm due to

$$\frac{)}{} v^2 \qquad (9)$$

ely, the thickness
see Figure 2), v is
ough the opening,
he opening divi-
s the number of
suming that the
side the gap, so
nduced pressure
sement and soil
re at the soil-gap

$$(T_s\text{-}T_b)z \qquad (10)$$

inate of the soil
ry conditions at
d by examining

Equation 7, we
velocity from
try rate, E_s, is

$$(11)$$

rea of the soil-
n integral over

tion in the soil

$$(r, z) \nabla C(r, z)\big]$$

$r, z) \qquad (12)$

---

where D is the bulk diffusivity of radon in soil, λ the radon decay constant, ε the porosity of the soil, and S the rate of release of radon into the soil gas per unit volume of soil. In this paper, we assume that the soil is homogeneous with $D = 10^{-6}$ m^2 s^{-1} and $\varepsilon = 0.5$ (Nazaroff, 1988a). The model does not deal with spatial variations in soil moisture; values of D, ε, and S may be chosen to reflect wet conditions. The boundary conditions for solution of Equation 12 are identical to those for Equation 7 except at the soil-gap interface. At the soil surface, we assume C = 0; because radon concentrations in soil gas are typically high compared to those in the atmosphere, the assumption of a non-zero soil-surface concentration has a negligible effect on the result. We assume that radon entry by diffusion through a gap is negligible compared to convective entry. In that case, the radon concentration immediately inside the gap is equal to that immediately outside, i.e., the normal derivative of C vanishes at the soil-gap interface. Other assumptions may be made, e.g., that the concentration inside an opening has an exponential profile, but the effect on the calculated radon entry rate is negligible in situations where the rate is high enough to produce elevated indoor concentrations (Loureiro, 1987; Loureiro et al., 1990).

The radon concentration at distances far from the soil surface and the basement, C_∞, is given by

$$C\infty = \frac{S}{\lambda} \qquad (13)$$

Since this paper does not deal with the soil characteristics that determine the radon source strength, we normalize C by C_∞, so that results are independent of S. From previously determined velocities and a solution to Equation 12, we find the normalized radon entry rate, E_r, from the equation

$$E_r = \frac{1}{C\infty} \int_\Sigma C(r, z)\vec{v}(r, z)\cdot d\vec{\sigma}(r, z) \qquad (14)$$

E_r has the dimensions of a volumetric flow rate, but must be distinguished from the soil-gas entry rate. Because the concentration at any opening is less than C_∞, E_r is always less than E_s.

The equations for the temperature, pressure, and concentration fields (1, 7, and 12) are each solved in the following manner. An irregular grid, similar to that of Loureiro (1987) divides the region into control volumes, which may vary greatly in size, and the equation of interest is integrated over each of the volumes using a first-order central difference scheme. The result is a set of difference equations of the form

$$C_{nm}\psi_{nm} = l_{nm}\psi_{n\text{-}1m} + r_{nm}\psi_{n+1m} + t_{nm}\psi_{nm\text{-}1}$$
$$+ b_{nm}\psi_{nm+1} + S_{nm} \qquad (15)$$

where ψ_{nm} represents the temperature, pressure, or radon concentration at the point (n,m), the coefficients c_{nm}, l_{nm}, r_{nm}, t_{nm}, and b_{nm} refer to the central, left, right, top, and bottom points, respectively, as viewed in the manner of Figure 1, and s_{nm} is the inhomogeneous part of the equation. These equations, with appropriate boundary conditions, are solved using iterative techniques described by Patankar (1980), Loureiro (1987), and Loureiro et al. (1990). The value of the field at iteration i, ψ_{nm}, is given by

$$\psi_{nm}^{*i} = \psi_{nm}^{*i\text{-}1} + \omega\left[\psi_{nm}^{i} - \psi_{nm}^{*i\text{-}1}\right] \qquad (16)$$

where $\psi^i{}_{nm}$ is the solutions of Equation 15 at iteration i, $\psi^{*i\text{-}1}{}_{nm}$ is the solution of Equation 16 at iteration i-1, and ω is the relaxation coefficient. Satisfactory results may generally be obtained for $\omega = 1.5$, except where temperature and pressure equations must be coupled, in which case ω must be taken less than 1 for numerical stability. All results cited in this paper have been obtained with $\omega = 1$.

Boundary values are introduced into Equation 15 in a straightforward manner; all have fixed values, except for the pressure at a

soil-gap interface, which requires special treatment. (The temperature and radon concentration at a soil-gap interface are treated conventionally. See Figure 2 and the discussions following Equations 1 and 12.) Let p_{nm} be the pressure at an interface node. Initially, we set ΔP_b to the representative winter value of -5 Pa and ΔP_g to zero; p_{nm} is found from the discrete form of Equation 4. After the first iteration, the pressure immediately outside the opening is known, and a relationship between this pressure, p_{nm}, and the average air speed at the opening can be found from the discrete form of Equation 5. A second expression involving p_{nm} and the average speed is Equation 9. From the two equations, a new value of p_{nm} is determined and used as a boundary value during the next iteration.

The temperature and pressure equations are solved simultaneously. The coefficients for each iteration of the temperature equation are calculated using velocities obtained from the previous iteration of the pressure equation. Similarly, the coefficients for each iteration of the pressure equation are calculated using temperatures obtained from the previous iteration of the temperature equation. The radon concentration equation is solved separately, its coefficients being calculated from velocities obtained from the final iteration of the pressure equation.

Iterations are permitted to continue until the residuals fall below a fixed tolerance; for results cited in this paper, the tolerance is 10^{-6}. As a further check when a gap is present, the total rate of mass transport through the gap is compared to the transport rate across the soil surface. For results cited in this paper, the relative difference is always less than 0.1%.

The final step in the procedure is the calculation of the soil-gas and radon entry rates, using the discrete forms of Equations 11 and 14.

Model Predictions

In this section, we compare the predictions of two-dimensional cylindrical and three-dimensional rectangular versions of the model, give a brief description of the nature and magnitude of the soil-gas flows and radon concentrations predicted by the model, and discuss the relationship between the radon entry rate, the indoor radon concentration, and the soil permeability for the configuration depicted in Figures 1 and 2. For a more complete discussion of the influence of soil permeability on radon entry, see Revzan, 1990. The influence of structural factors and construction practices on radon entry is the subject of Revzan and Fisk, 1990.

For the comparison of the two models, we assume that the configuration is that of Figures 1 and 2 and that the soil is homogeneous. In the simulations, the permeability varied from 10^{-12} to 10^{-10} m². The basement cross-section for the three-dimensional model was square; in two sets of simulations, the length of a side was first taken equal to the cylinder diameter d and then equal to $d/\sqrt{2}$, the latter value giving a diagonal equal to d. The gap width was 0.003 m. The discrepancies in the predicted soil-gas flux (i.e., entry rate per unit length of gap) were ~8% for all configurations, with the three-dimensional model making the lower prediction. The discrepancies in the radon concentration at the soil-gap interface were less than 1%, with the three-dimensional model predicting the higher value, so that the discrepancies in the predicted radon entry rate were on the order of 7%. Figure 3 shows the pressure immediately under the basement slab along the radius of the cylindrical cross-section and the half-diagonal of the square cross-section, both 5 m, for a basement pressure of -5 Pa. The slab-footer gap is 0.15 m from the wall, as shown in Figure 2. Generally, the three-dimensional model predicts a lower pressure gradient near the gap, and therefore a lower soil-gas entry rate than
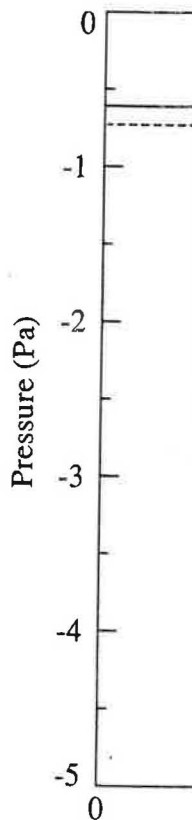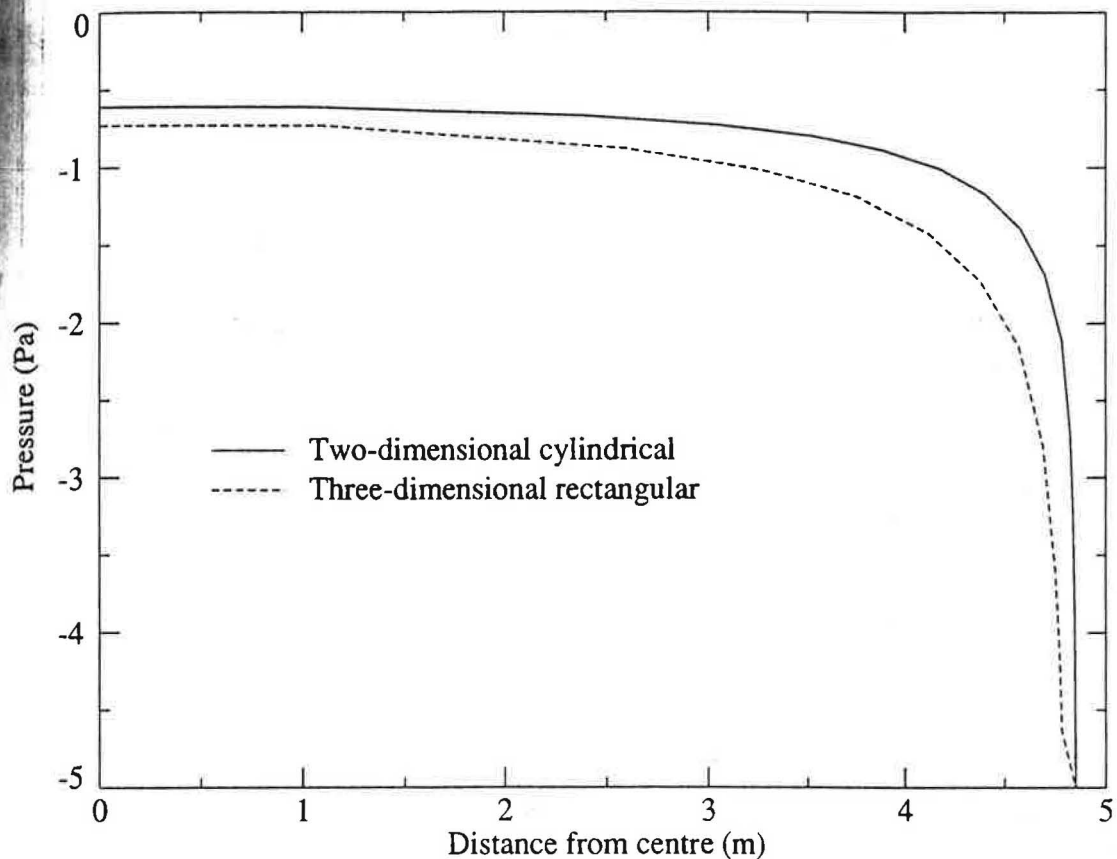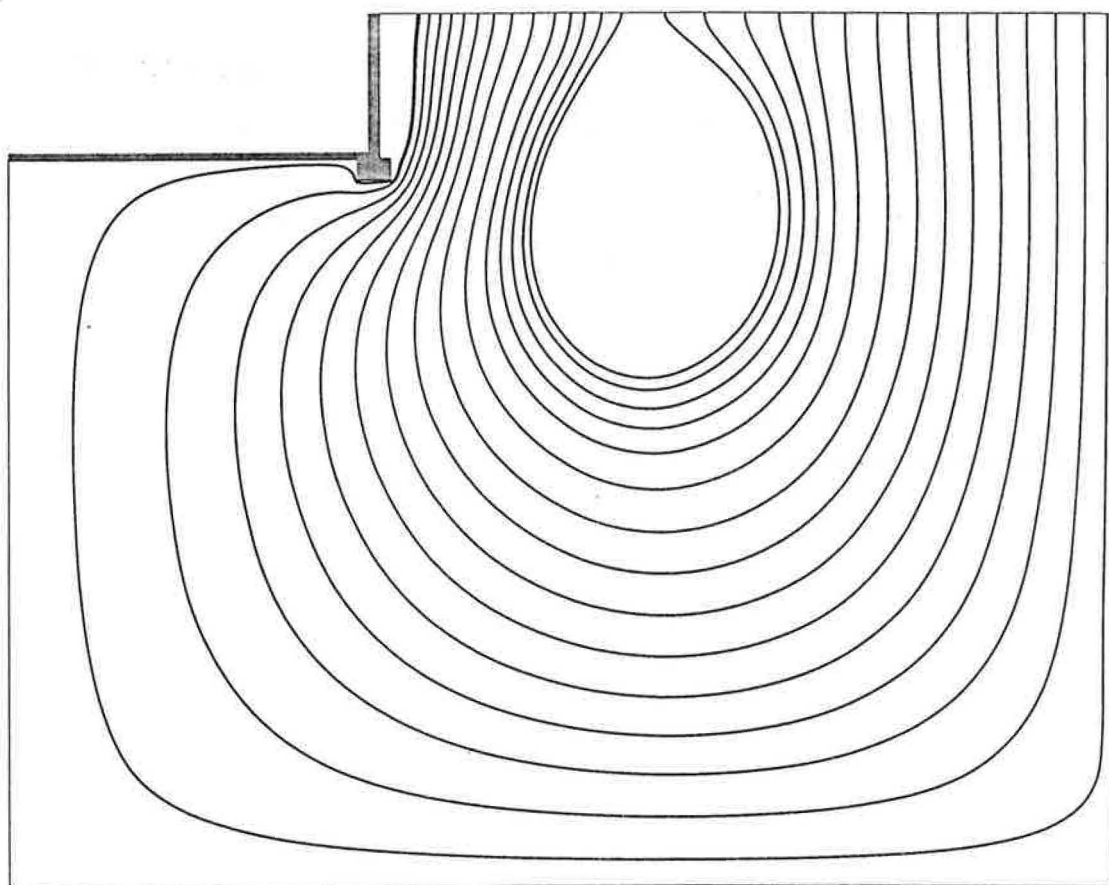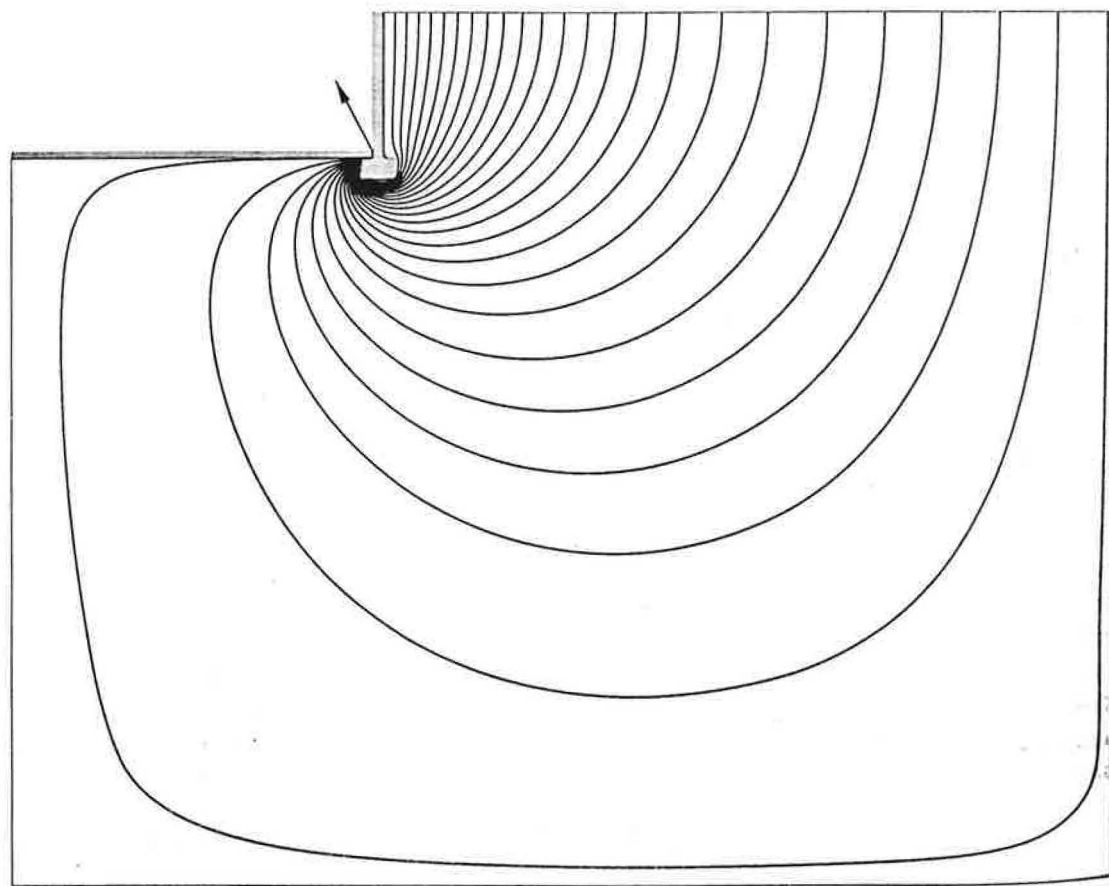

Fig. 3 Pressure imm... for the two-dimensio... sional rectangular m... Figures 1 and 2. The... mensional model ho... whose diagonal is e... cal horizontal cross-... model (10 m). The b... spect to the atmosph... slab-footer-wall gap... at the soil-gap interf... centre, is ~ -5 Pa a...

the cylindrical m... the square is les... fluxes predicted... nearly equal. Fi... relatively high... by the three-dir... ners of the foo... dients in these s... antly increase tl... or radon.

Fig. 3 Pressure immediately under the basement slab for the two-dimensional cylindrical and three-dimensional rectangular models. The configuration is that of Figures 1 and 2. The soil is homogeneous. The three-dimensional model has a square horizontal cross-section whose diagonal is equal to the diameter of the cylindrical horizontal cross-section of the two-dimensional model (10 m). The basement pressure is -5 Pa with respect to the atmosphere. The pressure drop across the slab-footer-wall gap is negligible, so that the pressure at the soil-gap interface, which is 4.85 m from the centre, is ~ -5 Pa as well.

are the predictions drical and three-dimensions of the model, of the nature and s flows and radon by the model, and between the radon ion concentration, for the configuration and 2. For a more e influence of soil ntry, see Revzan, ictural factors and radon entry is the , 1990.

ie two models, we ion is that of Figsoil is homogenthe permeability ². The basement hree-dimensional s of simulations, st taken equal to d then equal to ving a diagonal as 0.003 m. The ted soil-gas flux gth of gap) were with the threehe lower predice radon concente were less than nal model prethat the discredon entry rate re 3 shows the the basement he cylindrical iagonal of the m, for a baseib-footer gap is n in Figure 2. al model pre- near the gap, ntry rate than

the cylindrical model. Since the perimeter of the square is less than that of the circle, the fluxes predicted by the two models are more nearly equal. Figure 3 does not illustrate the relatively high pressure gradient predicted by the three-dimensional model at the corners of the footer; however, the high gradients in these small regions do not significantly increase the total entry rate of soil gas or radon.

The nature of the soil gas flows predicted by the cylindrical model may be seen in Figures 4-6, which show streamlines for the configuration of Figures 1 and 2. The soil temperature, where used, is determined by the model assuming an outside air temperature of 0 °C, a basement temperature of 15 °C, and a soil temperature at 10 m depth of 10 °C, which is the assumed annual mean, so that conditions are typical of winter in a cold climate. Figure 4 illustrates the case of pure natural convection. Here $\Delta P_b = 0$, i.e., the basement is at atmospheric pressure, so that the flow is a circulation toward the warmer basement wall. Figure 5 illustrates the case of pressure-driven flow for isothermal soil for a basement pressure 5 Pa lower than atmospheric. All flow lines run from the surface to the 0.003 m wide slab-footer opening,
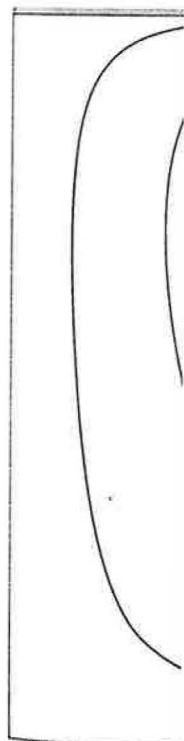
Fig. 4 Vertical cros
rounding soil, with
clockwise. In this c
between basemen
culation due to na
the basement, the
dary are 15, 0, an

Fig. 5 Vertical cros
rounding soil, with
clockwise. In this c
convection; the ba
the atmosphere.

Fig. 6 Vertical cros
rounding soil, with
clockwise. In this c
tion are present. Th
that of the atmosph
ment, the soil surfa
15, 0, and 10 °C, re

Fig. 4 Vertical cross-section of a basement and the surrounding soil, with streamlines; the direction of flow is clockwise. In this case there is no pressure difference between basement and outside, so that the flow is a circulation due to natural convection. The temperatures of the basement, the soil surface, and the lower soil boundary are 15, 0, and 10 °C, respectively.

Fig. 5 Vertical cross-section of a basement and the surrounding soil, with streamlines; the direction of flow is clockwise. In this case the flow is due entirely to forced convection; the basement pressure is 5 Pa below that of the atmosphere.

Fig. 6 Vertical cross-section of a basement and the surrounding soil, with streamlines; the direction of flow is clockwise. In this case both forced and natural convection are present. The basement pressure is 5 Pa below that of the atmosphere. The temperatures of the basement, the soil surface, and the lower soil boundary are 15, 0, and 10 °C, respectively.

which is the only gap in the basement shell. In Figure 6, the two cases are combined, so that both a circulation and a flow into the gap are present.

Normalized radon entry rates for the configuration of Figures 1 and 2 are plotted against the permeability of the homogeneous soil in Figure 7. The solid line shows the predicted entry rates for the complete model, with conduction and advection of heat included, i.e., with the temperature and pressure equations coupled. The basement, outside, and deep soil temperatures are 15, 0, and 10 °C, respectively. The dashed line shows the predicted results for isothermal conditions. For the soil permeabilities of greatest practical interest (10^{-10} – 10^{-12} m²), the introduction of thermal effects increases the radon entry rate by 35-40%. The dotted line
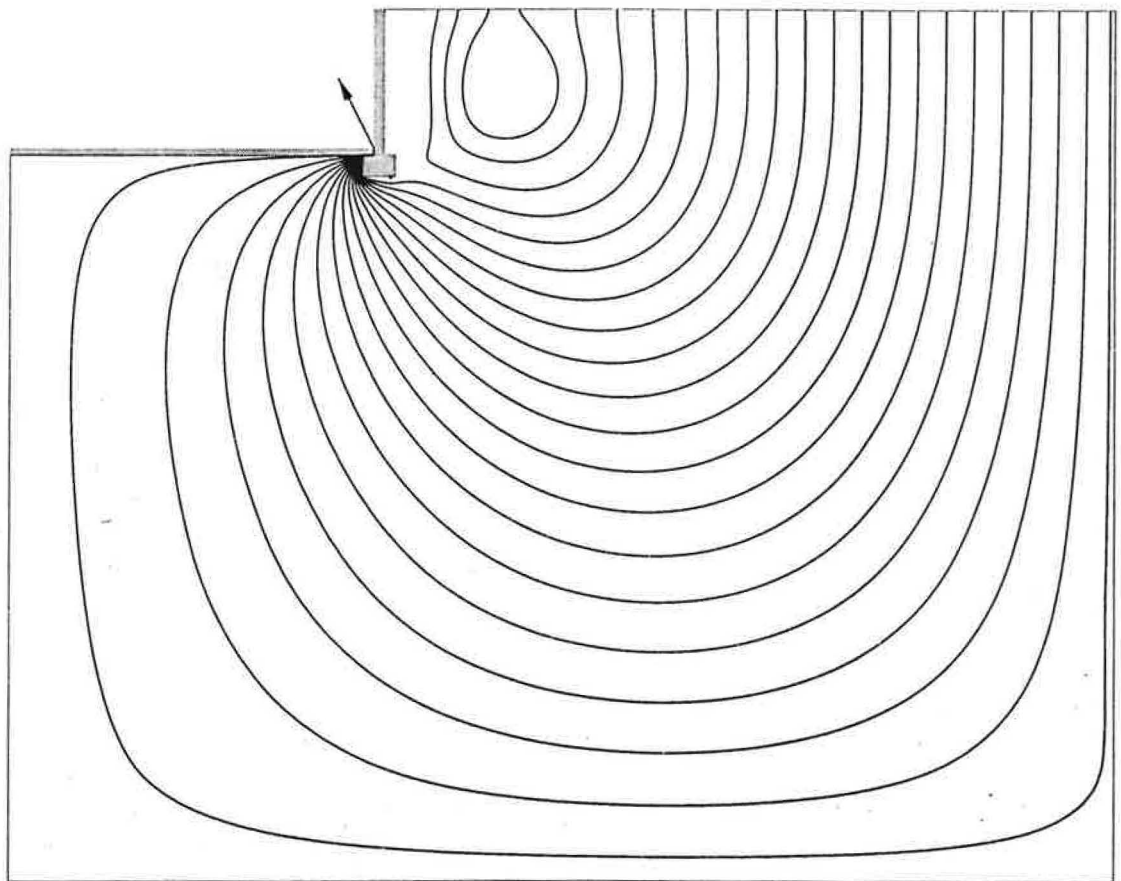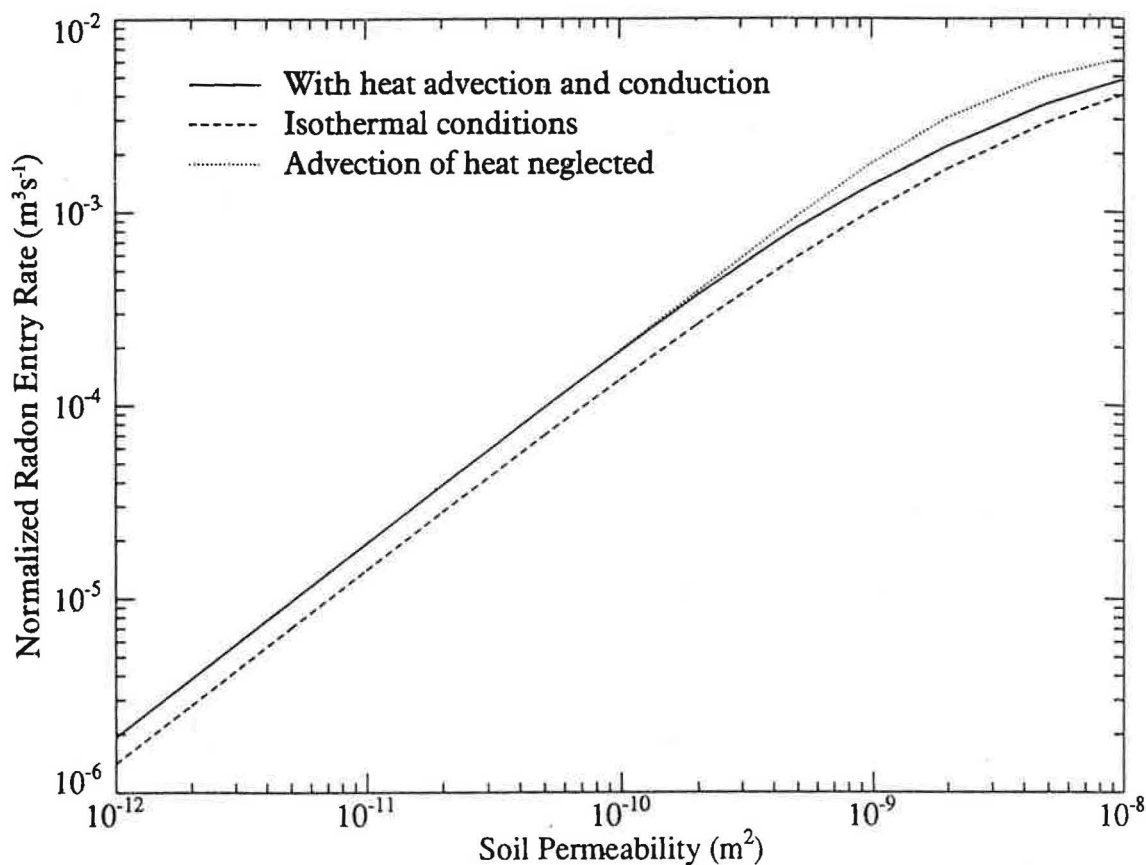
Fig. 7 The predicted normalized radon entry rate into the slab-footer gap of a basement, plotted against soil permeability, for the configuration of Figures 1 and 2. The basement is 5 Pa below atmospheric pressure. The solid line shows the predicted rates when both thermal conduction and convection are included in the model. The basement, outside, and deep soil temperatures are 15, 0, and 10 °C, respectively. The dashed line shows the predictions for isothermal conditions. The dotted line shows the predictions when thermal convection is neglected.

shows the predicted entry rates when heat advection is neglected but conduction is included. Advection of heat begins to become significant, for a basement pressure of -5 Pa, at a soil permeability of 10^{-10} m². Since the soil-gas speed is directly dependent on the product of $|\Delta P_b|$ and k, heat advection may be neglected when this product is less than $\sim 5 \times 10^{-10}$ Pa m².

The indoor radon concentration corresponding to a particular normalized entry rate depends on the radon concentration in the soil, the volume of the building, and the air-exchange rates between basement and outside, basement and living area, and living area and outside. A complete treatment of this subject is outside the scope of this paper, but in a simplified model in which the house is considered a single zone whose air is fully mixed, the indoor radon concentration, C, is given by
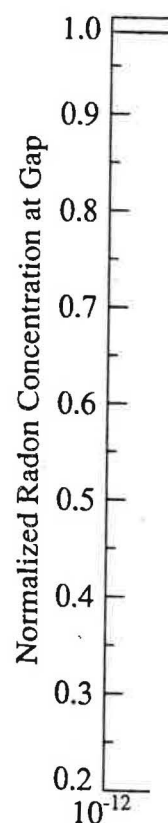
$$C = \frac{E_r C_\infty}{V\lambda} \tag{17}$$

where V and λ are, respectively, the volume and the exchange rate of the house. For a house of volume 500 m³ and air-exchange rate of 0.5 h⁻¹, whose surrounding soil has a

(typical) C_∞
must be mu
indoor rado
homogeneou
the predicte
Bq m⁻³. Wh
gravel is pr
the predicted
of 5 higher (

The relati
gas entry rat
approximate

$$E_r = E_s C_{avg}$$

where C_{avg} is
centration at
is linearly d
Figure 7 sho
between E_r a

(typical) C_∞ of 3.5×10^4 Bq m^{-3}, E_r (m^3 s^{-1}) must be multiplied by $\sim 5 \times 10^5$ to obtain the indoor radon concentration in Bq m^{-3}. For a homogeneous soil of permeability 10^{-11} m^2, the predicted indoor concentration is ~ 10 Bq m^{-3}. When a layer of high-permeability gravel is present under the basement slab, the predicted indoor concentration is a factor of 5 higher (Revzan and Fisk, 1990).

The relation between the radon and soil-gas entry rates at any narrow opening may be approximated by

$$E_r = E_s C_{avg} \tag{18}$$

where C_{avg} is the average soil-gas radon concentration at the opening. By Darcy's law, E_s is linearly dependent on soil permeability. Figure 7 shows, in contrast, that the relation between E_r and k is not linear, particularly at

high k. The departure from linearity is accounted for by the diminution in the radon concentration of the soil gas that enters the slab-footer gap as the soil permeability and soil-gas velocity increase. Figure 8 illustrates this point by showing the average normalized radon concentration at the slab-footer gap, plotted against the soil permeability, for the configuration of Figures 1 and 2.

Fig. 8 The predicted average normalized radon concentration in the slab-footer gap of a basement, plotted against soil permeability, for the configuration of Figures 1 and 2. The basement is 5 Pa below atmospheric pressure. The solid line shows the predicted concentrations when both thermal conduction and convection are included in the model. The basement, outside, and deep soil temperatures are 15, 0, and 10 °C, respectively. The dashed line shows the predictions for isothermal conditions. The dotted line shows the predictions when thermal convection is neglected.
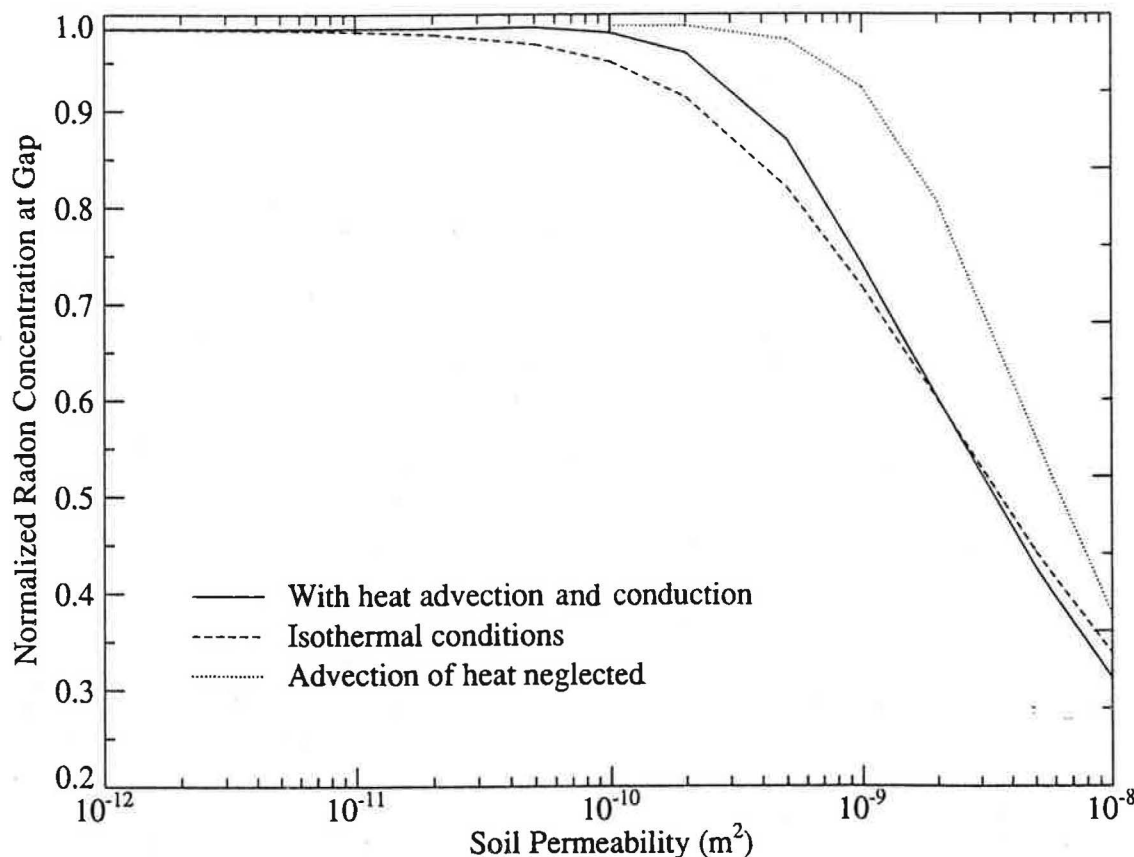
Model Verification

There are few data available to compare with the predictions of the model. However, a study of several houses in the Spokane River Valley of Washington and Idaho (Turk, et al., 1987) provides some information on permeabilities and entry rates for 14 houses, of which 6 had full concrete basements and one a basement and a small adjoining crawlspace. Since the results of permeability measurements are not precise, and since detailed information on the substructures and underlying soil are unavailable, we shall not discuss the houses individually, but rather compare the range of calculated entry rates with the predictions. The permeability of the soil underlying the entire area of the study appears to be on the order of 2×10^{-10} m^2. The normalized radon entry rates are calculated from the data provided by Turk from the equation

$$E_r = \frac{CV\lambda}{C\infty} \tag{19}$$

where C is the time-averaged indoor radon concentration in the living area, measured in the winter, λ is the time-averaged measured air-exchange rate, and C_∞ is based on analysis of soil samples taken far from the houses. For the seven houses which can be modelled reasonably well, the values of E_r calculated from measured data range from 5.5×10^{-4} to 3.2×10^{-3} m^3 s^{-1}; the mean and standard deviation are 1.7×10^{-3} and 1.1×10^{-3} m^3 s^{-1}, respectively. For a soil permeability of 2×10^{-10} m^2, no subslab gravel layer (no layer having been reported), and a slab-footer gap width of 0.003 m, the model predicts an entry rate of 3.8×10^{-4} m^3 s^{-1} when the basement-outside pressure difference is a nominal winter value of -5 Pa (Revzan, et al., 1988; Revzan, 1989) and the basement, soil surface, and lower soil boundary temperatures are 15, 0, and 10 °C, respectively.

The predicted entry rate is 22% of the calculated mean; the discrepancy may be accounted for by inadequacies in the measurement of permeability. Some soils exhibit anisotropy in permeability (Nazaroff, 1988a), the permeability for airflow parallel to the soil surface being greater than that for flow perpendicular to the surface. It is unclear whether the measured permeability represents the permeability in one of the two directions or an average of the two. Furthermore, since the permeability measurements were made during the rainy season, it is possible that the average winter permeabilities exceed the measured value; permeability measured in water-saturated soil can easily be 0.3 of the dry value or even less (Nazaroff, 1988a). Perhaps more significantly, the errors in the measurements of soil permeability may be high. The assumption of a soil permeability of 1.4×10^{-9} m^2, a factor of 7 greater than the measured value, leads to a predicted entry rate approximately equal to the mean of the values determined from the data.

On the other hand, the discrepancy will be larger if the average $|\Delta P_b|$ is smaller than 5 Pa, if the basement-outside temperature difference is smaller than 15 °C, if the gap width is less than 0.003 m, if the soil block from which each house may draw radon is smaller than we have estimated or if the entry rates have been underestimated. The entry rates were calculated from radon concentrations measured in the living areas on the assumption that forced-air furnaces (present in 5 of the 7 houses) assured good mixing of air in most of the houses. If basement radon levels were significantly higher than those upstairs, then the entry rates calculated from Equation 19, with C equal to the basement concentration, would be higher than the stated values.

The highest and lowest entry rates determined from measurements differ by a factor of 6. Since the regression of the entry rate on the permeability has an R^2 of 0.01, the disparity cannot be accounted for by differences in soil permeabilities, and we must infer that there are differences in structures, sites, and soils which have not been taken into ac-

count. A peripher[...] shell is a norma[...] practices. Additio[...] the result of pen[...] cracking of the co[...] nation of the pred[...] that the addition[...] ily to redistribute[...] increasing the ove[...] 1.5 at most (Revz[...] may also enter[...] walls (Garbesi an[...]

Although it is[...] placed under a s[...] well drained (i.e.,[...] be that a gap betw[...] bance of the soil[...] a high-permeabil[...] The assumption[...] 2×10^{-10} m^2 everyw[...] permeability 10^{-9} a[...] the slab leads to[...] 9.0×10^{-4} m^3 s^{-1}, wh[...] the entry rates cal[...] entry rate remains[...] when the thickne[...] the permeability[...] ches infinity, so t[...] the concrete slab a[...] fused with the slab[...] approaches 1.3×10^{-3}[...] mean. If the thicl[...] the slab-footer ga[...] entry rate is 1.2×10[...]

In sum, the ra[...] slab-footer gap pr[...] suming a homoge[...] considerably lowe[...] inferred from me[...] pancy may be ac[...] take into account[...] underestimation[...] regions immediate[...] the building shell.[...] ence of permeable[...] ings in the buildin[...]

ne soils exhibit ani-
Nazaroff, 1988a), the
parallel to the soil
n that for flow per-
. It is unclear whe-
leability represents
f the two directions
Furthermore, since
ements were made
it is possible that
abilities exceed the
ility measured in
asily be 0.3 of the
zaroff, 1988a). Per-
the errors in the
meability may be
a soil permeability
7 greater than the
a predicted entry
o the mean of the
e data.

iscrepancy will be
| is smaller than
side temperature
15 °C, if the gap
, if the soil block
ay draw radon is
ated or if the en-
timated. The en-
m radon concen-
ing areas on the
urnaces (present
l good mixing of
basement radon
gher than those
calculated from
to the basement
ier than the sta-

try rates deter-
iffer by a factor
he entry rate on
0.01, the dispar-
y differences in
nust infer that
ires, sites, and
taken into ac-

count. A peripheral opening in the basement
shell is a normal consequence of building
practices. Additional openings may exist as
the result of penetrations for utilities or of
cracking of the concrete. However, an exami-
nation of the predictions of the model shows
that the addition of openings serves primar-
ily to redistribute the flow of soil gas while
increasing the overall entry rate by a factor of
1.5 at most (Revzan and Fisk, 1990). Radon
may also enter through permeable block
walls (Garbesi and Sextro, 1990).

Although it is not usual for gravel to be
placed under a slab when the soil itself is
well drained (i.e., highly permeable), it may
be that a gap between slab and soil or distur-
bance of the soil during construction creates
a high-permeability region under the slab.
The assumption of a soil permeability of
2×10^{-10} m^2 everywhere except for a region of
permeability 10^{-9} and thickness 0.15 m under
the slab leads to a predicted entry rate of
9.0×10^{-4} m^3 s^{-1}, which is 53% of the mean of
the entry rates calculated from the data. The
entry rate remains high (5.8×10^{-4} m^3 s^{-1}) even
when the thickness is as low as 0.01 m. As
the permeability of the 0.01 m layer approa-
ches infinity, so that there is a gap between
the concrete slab and the soil (not to be con-
fused with the slab-footer gap), the entry rate
approaches 1.3×10^{-3} m^3 s^{-1}, which is 76% of the
mean. If the thickness is reduced to that of
the slab-footer gap itself, i.e., 0.003 m, the
entry rate is 1.2×10^{-3} m^3 s^{-1}.

In sum, the radon entry rate through a
slab-footer gap predicted by the model, as-
suming a homogeneous and isotropic soil, is
considerably lower than the total entry rate
inferred from measured data. The discre-
pancy may be accounted for by failure to
take into account permeability anisotropy,
underestimation of the permeability of the
regions immediately adjacent to openings in
the building shell, and by the possible pres-
ence of permeable walls and additional open-
ings in the building shell.

Summary and Conclusions

We have modified the three-dimensional
steady-state model of Loureiro et al. (1990) to
simulate pressure and radon concentration
fields in the vicinity of a cylindrically-sym-
metrical representation of a basement. The
boundaries of the simulation space are the
outside of the basement wall, slab, and footer,
the mouth of the slab-footer gap, and the
outer limits of the soil block associated with
the basement. The basement may be warmer
than the soil and the outside; natural convec-
tion (buoyancy) of soil gas resulting from
this condition is included in the model, and
has been shown to increase radon entry by
approximately 40%. Three important sub-
jects have not been examined. First, the ef-
fects of temporal variations in barometric
pressure, which may be far greater in ampli-
tude than the steady-state basement-outside
pressure differences, have been neglected. A
time-dependent model is being developed to
determine whether these effects, which may
be significant when the soil permeability is
low, are an important factor in radon entry.
Second, we have neglected soil moisture,
which affects both soil permeability and
soil-gas radon concentration. Moisture is cer-
tainly an important factor in the production
and transport of radon in soil, and the exten-
sion of the model to deal with its influence,
even in an unsophisticated manner, is clearly
necessary. Third, permeability anisotropy
has been neglected. The model is being mod-
ified to permit the permeability to be treated
as a tensor, rather than as a scalar.

In a comparison of radon entry rates pre-
dicted by the model with those determined
from a study of the Spokane, WA region, we
have chosen values of the basement pressure
and temperature that are typical of winter in
cold regions and soil permeabilities that are
close to those measured. If the soil is as-
sumed to be homogeneous and isotropic,
with permeability equal to the mean of the
measured values, the predicted radon entry

rate is 22% of the mean of the observations. The observed radon entry rates may then be accounted for by assuming that a narrow gap exists between the basement slab and the soil, by assuming that there are gaps in the basement shell in addition to the slab-footer gap, and by taking the soil permeability to be somewhat higher than the measured value, which is highly uncertain. Further verification of the model requires a more completely characterized site and the maintenance of steady-state conditions; work on an experimental structure that meets these conditions is now proceeding (Fisk et al., 1989).

Acknowledgements

References

Baker, P.H., Sharples, S. [...] through cracks", Bui[...] 293-304.

Bejan, A. (1984) Convectio[...] ley.

Dimbylow, P.J. (1987) "T[...] ven flow equation for [...] concrete foundations" [...] 18(3), 163-167.

Ene, H.I. and Polisevski [...] ous Media, Dordrecht, [...]

Feustel, H.E. and Sherr[...] model for predicting [...] tures", Energy and Bui[...]

Fisk, W.J., Flexser, S., G[...] era, M.P., Narasimh[...] K.L., Sextro, R.G., Sm[...] lenberg, H.A. (1989) [...] don Entry into Baseme[...] Structures Project, Lav[...] port LBL-27962.

Garbesi, K. and Sextro, [...] evidence of pressure-[...] house through perm[...] onmental Science and [...]

Loureiro, C.O. (1987) [...] Transport of Radon fro[...] under Constant Negat[...] Laboratory Report L[...]

Loureiro, C.O., Abriola[...] R.G. (1990) "Three [...] transport into house[...] sure", Environmental [...] 1348.

Mowris, R.J. and Fisk, [...] of exhaust ventilatio[...] radon concentrations[...]

Nazaroff, W.W. (1988a) [...] generation, migratio[...] and Nero, A.V., (eds[...] Indoor Air, New Yor[...]

References

Baker, P.H., Sharples, S. and Ward, I.C. (1989) "Air flow through cracks", *Building and Environment*, 22(4), 293-304.

Bejan, A. (1984) *Convection Heat Transfer*, New York, Wiley.

Dimbylow, P.J. (1987) "The solution of the pressure driven flow equation for radon ingress through cracks in concrete foundations", *Radiation Protection Dosimetry*, 18(3), 163-167.

Ene, H.I. and Polisevski, D. (1987) *Thermal Flow in Porous Media*, Dordrecht, Reidel.

Feustel, H.E. and Sherman, M.H. (1989) "A simplified model for predicting air flow in multizone structures", *Energy and Buildings*, 13, 217-230.

Fisk, W.J., Flexser, S., Gadgil, A.J., Holman, H.-Y., Modera, M.P., Narasimhan, T.N., Nuzum, T., Revzan, K.L., Sextro, R.G., Smith, A.R., Tsang, Y.W. and Wollenberg, H.A. (1989) *Monitoring and Modelling for Radon Entry into Basements: A Status Report for the Small Structures Project*, Lawrence Berkeley Laboratory Report LBL-27962.

Garbesi, K. and Sextro, R.G. (1990) "Modeling and field evidence of pressure-driven entry of soil gas into a house through permeable below-grade walls", *Environmental Science and Technology*, 23, 1481-1487.

Loureiro, C.O. (1987) *Simulation of the Steady-State Transport of Radon from Soil into Houses with Basements under Constant Negative Pressure*, Lawrence Berkeley Laboratory Report LBL-24378.

Loureiro, C.O., Abriola, L.M., Martin, J.E. and Sextro, R.G. (1990) "Three dimensional simulation of radon transport into houses under constant negative pressure", *Environmental Science and Technology*, 24, 1338-1348.

Mowris, R.J. and Fisk, W.J. (1987) "Modelling the effects of exhaust ventilation on radon entry rates and indoor radon concentrations", *Health Physics*, 54, 491-501.

Nazaroff, W.W. (1988a) "Soil as a source of indoor radon: generation, migration, and entry". In: Nazaroff, W.W. and Nero, A.V., (eds), *Radon and its Decay Products in Indoor Air*, New York, Wiley, pp. 57-112.

Nazaroff, W.W. (1988b) "Predicting the rate of ^{222}Rn entry from soil into the basement of a dwelling due to pressure-driven air flow", *Radiation Protection Dosimetry*, 24(1), 199-202.

Nero, A.V. (1988) "Radon and its decay products in indoor air: an overview". In: Nazaroff, W.W. and Nero, A.V., (eds), *Radon and its Decay Products in Indoor Air*, New York, Wiley, pp. 1-53.

Oke, T.R. (1987) *Boundary Layer Climates*, New York, Methuen.

Patanker, S.V. (1980) *Numerical Heat Transfer and Fluid Flow*, New York, Hemisphere.

Revzan, K.L. (1989) *Radon Entry, Distribution, and Removal in Two New Jersey Houses with Basements*, Lawrence Berkeley Laboratory Report LBL-26830.

Revzan, K.L. (1990) *Modelling Radon Entry into Houses with Basements: the Influence of Soil Characteristics*, Lawrence Berkeley Laboratory Report LBL-28109.

Revzan, K.L. and Fisk, W.J. (1990) *Modelling Radon Entry into Houses with Basements: the Influence of Structural Factors*, Lawrence Berkeley Laboratory Report LBL-28267 (submitted to Indoor Air).

Revzan, K.L., Turk, B.H., Harrison, J., Nero, A.V. and Sextro, R.G. (1988) "Parametric modelling of temporal variations in radon concentrations in homes", *IEEE Transactions in Nuclear Science*, 35(1), 550-555.

Sherman, M.H., Grimsrud, D.T. and Diamond, R.C. (1979) *Infiltration-Pressurization Correlation: Surface Pressures and Terrain Effects*, Lawrence Berkeley Laboratory Report LBL-8785.

Turk, B.H., Prill, R.J., Grimsrud, D.T., Moed, B.A. and Sextro, R.G. (1987) *Radon and Remedial Action in Spokane Valley Homes, Volume I: Experimental Design and Data Analysis*, Lawrence Berkeley Laboratory Report LBL-23430.

Zapalac, G.H. (1983) "A time-dependent method for characterizing the diffusion of Radon-222 in concrete", *Health Physics*, 45(2), 377-283.